Eur. Phys. J. C 52, 451–457 (2007)
DOI 10.1140/epjc/s10052-007-0371-y

THE EUROPEAN PHYSICAL JOURNAL C

Regular Article – Theoretical Physics

Probing noncommutative space-time in the laboratory frame

Jun-ichi Kamoshita[a]

Institute of Humanities and Sciences and Department of Physics, Ochanomizu University, 2-1-1 Otsuka, Bunkyo, Tokyo 112-8610, Japan

Received: 15 June 2002 / Revised version: 31 May 2006 /
Published online: 3 August 2007 –

Abstract. The phenomenological investigation of noncommutative space-time in the laboratory frame is presented. We formulate the apparent time variation of noncommutativity parameter $\theta_{\mu\nu}$ in the laboratory frame due to the earth's rotation. Furthermore, in the noncommutative QED, we discuss how to probe the electric-like component $\theta_{\mathbf{E}} = (\theta_{01}, \theta_{02}, \theta_{03})$ by the process $e^-e^+ \to \gamma\gamma$ at future e^-e^+ linear collider. We may determine the magnitude and the direction of $\theta_{\mathbf{E}}$ by detailed study of the apparent time variation of the total cross-section. If no signal is observed, the upper limit on the magnitude of $\theta_{\mathbf{E}}$ can be determined independent of its direction.

1 Introduction

The early study of noncommutative space-time was presented by Snyder [1, 2] in 1947, with respect to the need to regularize the divergence of quantum field theory. In Snyder's work, it was suggested that the divergence may be regularized by an elementary unit of length induced by the noncommutativity of space-time. Snyder's basic idea was the extension of the quantization of phase space in quantum mechanics. Furthermore, noncommutativity of space-time may arise from string theory in the specific low energy limit [3, 4]. The noncommutative space-time is characterized by operators $\hat{X}_\mu$ satisfying the commutation relation

$$[\hat{X}_\mu, \hat{X}_\nu] = \mathrm{i}\theta_{\mu\nu}\,, \tag{1}$$

where $\theta_{\mu\nu}$ is antisymmetric constant matrix, $\theta_{\mu\nu} = -\theta_{\nu\mu}$ and $[\hat{X}_\rho, \theta_{\mu\nu}] = 0$, and $\theta_{\mu\nu}$ have dimension of $(\mathrm{Length})^2$. Therefore, (1) introduces the elementary unit of length in the theory, such as the Planck constant in quantum mechanics.

Nonzero constant matrix $\theta_{\mu\nu}$ may violate Lorentz invariance. Lorentz violations have been studied in noncommutative quantum field theory [5] and also in the framework of an effective Lagrangian in which Lorentz and CPT invariance are violated [6–8].

It is known that QED in noncommutative space time (NCQED) [9] is invariant under the noncommutative version of U(1) gauge transformation and is renormalizable at one loop level [9–12]. Axial anomaly [11, 12] and CPT invariance [13] in NCQED have also been studied. There are several phenomenological studies on NCQED for low energy experiments [14–19]. Assuming $\theta_{\mu\nu}$ is constant in the laboratory frame, researchers have found the noncommutativity scale Λ_{NC} to satisfy $\Lambda_{\mathrm{NC}} > 100\,\mathrm{GeV}$ [18], so that the result of Lamb shift is consistent with the ordinary quantum mechanics. Other limits on noncommutativity parameter have been found to be $\theta \lesssim (10\,\mathrm{TeV})^{-2}$, if $\theta_{\mu\nu} \equiv \theta\epsilon_{\mu\nu}$, by an analysis of noncommutative Aharonov–Bohm effect [19]. High energy phenomenology in NCQED has also been studied for several processes at future linear colliders [20–26]. Moreover, phenomenology relevant to standard model (SM) like interactions in noncommutative space-time have also been studied [27–38] on the assumption that we may obtain SM-like interaction in noncommutative space-time by the procedure replacing every products of fields with the star product. In those previous studies, however, the direction of $\theta_{\mu\nu}$ have been assumed to be fixed to the laboratory frame. Such an assumption might be justified, if measurements would be given by the data set suitably averaged over time and also over polar angle distributions.

The $\theta_{\mu\nu}$, however, may be considered as an elementary constant in the nature. And there may exist a class of specific coordinate system in which the direction of $\theta_{\mu\nu}$ is fixed. It is likely that such a coordinate system is fixed to the celestial sphere.

On the contrary, the laboratory frame is located on the earth and is moving by the earth's rotation. Therefore, as was mentioned in [20, 38, 39], we should take into account the apparent time variation of $\theta_{\mu\nu}$ in the laboratory frame due to the earth's rotation when we discuss phenomenology for any experiment on the earth. In this paper, we will consider the effect of apparent time variation of $\theta_{\mu\nu}$ in the collider experiments by taking the earth's rotation seriously.

If an anisotropy due to noncommutativity of space-time exists, probing the specific direction of $\theta_{\mu\nu}$ and measur-

[a] e-mail: kamosita@sofia.phys.ocha.ac.jp

ing the magnitude of elementary unit of length are very interesting tasks from both experimental and theoretical aspects. We may determine the direction of $\theta_{\mu\nu}$ by the analysis taking into account effects of time variation of the measurements.

This paper is organized as follows. In Sect. 2, we present the parameterization of $\theta_{\mu\nu}$, including the effect of the earth's rotation. In Sect. 3, we make some comments on the time dependent cross-section and we define the time averaged cross-section. In Sect. 4, we show several numerical results and we discuss how to probe $\theta_{\mu\nu}$ at future linear collider experiments. Finally, we conclude our result and discussion.

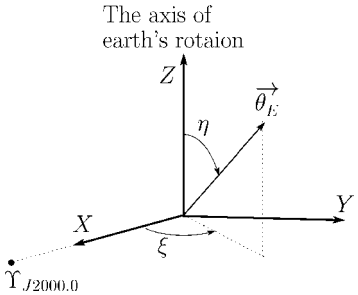

Fig. 1. The "primary" coordinate system (X–Y–Z). The axis X point to the vernal equinox $\Upsilon_{J2000.0}$. The electric-like component $\theta_{\mathbf{E}}$ of $\theta_{\mu\nu}$ is also shown. The direction of $\theta_{\mathbf{E}}$ is parameterized by the polar angle η and the azimuth ξ

2 Expression of $\theta_{\mu\nu}$ in the laboratory frame

The noncommutativity parameter $\theta_{\mu\nu}$ can be classified into two parts. One is the electric-like component $\theta_{\mathbf{E}} = (\theta_{01}, \theta_{02}, \theta_{03})$. Another is the magnetic-like component $\theta_{\mathbf{B}} = (\theta_{23}, \theta_{31}, \theta_{12})$. Those elements can be determined when a coordinate system is chosen. In the specific coordinate system, both $\theta_{\mathbf{E}}$ and $\theta_{\mathbf{B}}$ should be constant vectors. Hereafter we call such a coordinate system a "primary" coordinate system. It is feasible that we take a set of coordinates fixed to the rest frame of the cosmic microwave background(CMB) as a "primary" coordinate system. According to COBE experiment [40, 41], the boost of the solar system for the CMB rest frame is about 370 km/s. This is about 0.12% of the speed of light in a vacuum. Moreover the speed of the earth in the solar system is about 29.78 km/s. Therefore the effect of the boost to the measurement of $\theta_{\mathbf{E}}$ and $\theta_{\mathbf{B}}$ are small enough to be neglected in comparison with the detector resolution in the collider experiments. And we may consider that the CMB rest frame is fixed to the celestial sphere approximately. Thus, hereafter, we assume that a primary coordinate system and also each direction of $\theta_{\mathbf{E}}$ and $\theta_{\mathbf{B}}$ are fixed to the celestial sphere effectively.

First, we introduce a primary coordinate system. The Z axis is along the axis of the earth's rotation and the positive direction of Z axis points to the north. The axis pointed to the vernal equinox ($\Upsilon_{J2000.0}$) is labeled X. We take the X–Y–Z system as the right-hand system. Figure 1 shows the sketches of the primary coordinate system and the direction $\theta_{\mathbf{E}}$ parametrized by η and ξ.

Let $\mathbf{e_X}$, $\mathbf{e_Y}$ and $\mathbf{e_Z}$ be the orthonormal basis of the primary coordinate system (X–Y–Z). Then

$$\theta_{\mathbf{E}} = \theta_E \left(\mathbf{e_X} \sin\eta\cos\xi + \mathbf{e_Y} \sin\eta\sin\xi + \mathbf{e_Z}\cos\eta\right) , \tag{2}$$

where $0 \le \eta \le \pi$, $0 \le \xi \le 2\pi$ and $\theta_E \equiv |\theta_{\mathbf{E}}|$. To be exact, this X–Y–Z coordinate system moves slightly owing to the earth's precession. Since the period of the earth's precession is about 2.6×10^4 years, the vernal equinox is moving by about 0.014 degree/year. Therefore, we can neglect the earth's precession during the term of most experiments.

On the other hand, the usual coordinate system for experiments is fixed to the detector. We label each axis of such a coordinate system by small letter (x, y, z). As an example we consider an e^-e^+ collider experiment. The origin is set at the interaction point. The z axis is along the direction of the e^- beam. The y axis is chosen along the zenith and the x axis is chosen along the horizontal direction to make a right-hand coordinate. Hereafter we call this coordinate system the "laboratory" coordinate system.

As is shown in Fig. 2, we parameterize the orientation of an e^-e^+ experiment on the earth by an angle δ between the y axis and the X–Y plane at the interaction point[1], the angle a between the z axis direction and the meridian at the detector site, and the angle ζ between the X–Z plane and y–Z plane. The angle a is measured counterclockwise from the north.[2]

Let $\mathbf{e_x}$, $\mathbf{e_y}$ and $\mathbf{e_z}$ be the orthonormal basis of the laboratory coordinate system (x–y–z). The transformation between $(\mathbf{e_X}, \mathbf{e_Y}, \mathbf{e_Z})$ and $(\mathbf{e_x}, \mathbf{e_y}, \mathbf{e_z})$ is given by

$$\begin{pmatrix} \mathbf{e_X} \\ \mathbf{e_Y} \\ \mathbf{e_Z} \end{pmatrix} = R \begin{pmatrix} \mathbf{e_x} \\ \mathbf{e_y} \\ \mathbf{e_z} \end{pmatrix} , \tag{3}$$

$$\begin{aligned} R &= \begin{pmatrix} c_\zeta & -s_\zeta & 0 \\ s_\zeta & c_\zeta & 0 \\ 0 & 0 & 1 \end{pmatrix} \begin{pmatrix} c_\delta & 0 & -s_\delta \\ 0 & 1 & 0 \\ s_\delta & 0 & c_\delta \end{pmatrix} \begin{pmatrix} 1 & 0 & 0 \\ 0 & c_a & -s_a \\ 0 & s_a & c_a \end{pmatrix} \\ &\quad \times \begin{pmatrix} 0 & 1 & 0 \\ -1 & 0 & 0 \\ 0 & 0 & 1 \end{pmatrix} \\ &= \begin{pmatrix} c_a s_\zeta + s_\delta s_a c_\zeta & c_\delta c_\zeta & s_a s_\zeta - s_\delta c_a c_\zeta \\ -c_a c_\zeta + s_\delta s_a s_\zeta & c_\delta s_\zeta & -s_a c_\zeta - s_\delta c_a s_\zeta \\ -c_\delta s_a & s_\delta & c_\delta c_a \end{pmatrix} , \end{aligned} \tag{4}$$

with $-\pi/2 \le \delta \le \pi/2$ and $0 \le a \le 2\pi$, where we use the usual abbreviation, $c_\zeta = \cos\zeta$, etc.

In the study of Lorentz violation [6, 7], a similar transformation was considered. By setting $\delta = 0$ and replac-

[1] The δ may be regarded as the latitude of the detector site approximately.

[2] Our definition of the angle a is opposite to the definition of the azimuth in astronomy. We define the angle a as it increases with a positive rotation in the right-hand system. We may call the angle a the counter-azimuth.

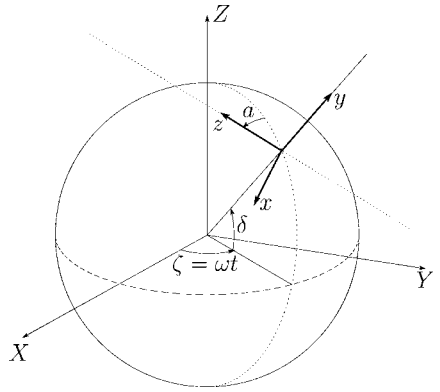

Fig. 2. Arrangement of laboratory coordinate system (x–y–z) for an experiment on the earth in the "primary" coordinate system (X–Y–Z). δ, a and ω are constants

ing ζ to $\zeta+\pi/2$ in (4), we can reproduce the transformation formula used in [6, 7]. The difference between the two parametrizations is mainly in the definition of the laboratory coordinate system, especially y axis. In [6, 7], the y axis is always taken to be parallel to the X–Y plane in the primary coordinate system. Hence the x and y axes in [6, 7] are different from those in the collider experiments. Our parametrization of the x, y, z axes can be readily used in any collider or accelerator experiments whose beams are set parallel to the earth surface.

Hereafter we take the orthonormal basis of the laboratory coordinate system as the usual way, $\mathbf{e_x} = (1,0,0)^T$, $\mathbf{e_y} = (0,1,0)^T$ and $\mathbf{e_z} = (0,0,1)^T$. Then, in the laboratory coordinate system, the orthonormal basis of the primary coordinate system can be written as

$$\mathbf{e_X} = \begin{pmatrix} c_a s_\zeta + s_\delta s_a c_\zeta \\ c_\delta c_\zeta \\ s_a s_\zeta - s_\delta c_a c_\zeta \end{pmatrix} ,$$
$$\mathbf{e_Y} = \begin{pmatrix} -c_a c_\zeta + s_\delta s_a s_\zeta \\ c_\delta s_\zeta \\ -s_a c_\zeta - s_\delta c_a s_\zeta \end{pmatrix} ,$$
$$\mathbf{e_Z} = \begin{pmatrix} -c_\delta s_a \\ s_\delta \\ c_\delta c_a \end{pmatrix} . \tag{5}$$

Note that in the laboratory coordinate system the direction of Z axis, namely the axis of the earth's rotation, is fixed by the location and the orientation of e^-e^+ experiment (δ, a). For example, (δ, a) of LEP experiments [42] are approximately (46.15°, 40°) for OPAL, (46.15°, 130°) for ALEPH, (46.15°, 220°) for L3 and (46.15°, 310°) for DELPHI.

The angle ζ increases with time t owing to the earth's rotation. A detector site will return to the same direction by a sidereal day, $T_{\rm day} = 23\,\mathrm{h}56\,\mathrm{m}4.09053\,\mathrm{s}$ [43]. Therefore, we may take

$$\zeta = \omega t \quad \text{with} \quad \omega \equiv 2\pi/T_{\rm day} , \tag{6}$$

by setting $t = 0$ when the detector site is on the X–Z half plane with $X > 0$. In this way, all the experimental data at all times can be combined by keeping the right phase.

Substituting (5) into (2), we find the expression of $\theta_{\mathbf{E}}$ in the laboratory coordinate system,

$$\theta_{\mathbf{E}} = \theta_{\mathbf{EV}} + \theta_{\mathbf{ES}} , \tag{7}$$
$$\theta_{\mathbf{EV}} = \theta_E \sin\eta \left[\begin{pmatrix} s_\delta s_a \\ c_\delta \\ -s_\delta c_a \end{pmatrix} c_{(\omega t-\xi)} + \begin{pmatrix} c_a \\ 0 \\ s_a \end{pmatrix} s_{(\omega t-\xi)} \right] , \tag{8}$$
$$\theta_{\mathbf{ES}} = \theta_E \cos\eta \begin{pmatrix} -c_\delta s_a \\ s_\delta \\ c_\delta c_a \end{pmatrix} , \tag{9}$$

where $\theta_{\mathbf{ES}}$ is the projection of $\theta_{\mathbf{E}}$ onto the Z axis and is the stable part of $\theta_{\mathbf{E}}$ in the laboratory coordinate system. $\theta_{\mathbf{EV}}$ is the time variation part of $\theta_{\mathbf{E}}$. The direction of $\theta_{\mathbf{EV}}$ revolves about the $\theta_{\mathbf{ES}}$ axis by a period $T_{\rm day}$. This is the apparent time variation due to the earth's rotation. The angle parameter ξ appears in the expression of $\theta_{\mathbf{EV}}$ as the initial phase for time evolution. It is easy to show that

$$|\theta_{\mathbf{ES}}| = |\theta_{\mathbf{E}}| \cos\eta , \quad |\theta_{\mathbf{EV}}| = |\theta_{\mathbf{E}}| \sin\eta ,$$
$$\theta_{\mathbf{ES}} \cdot \theta_{\mathbf{EV}} = 0 , \quad |\theta_{\mathbf{ES}}|^2 + |\theta_{\mathbf{EV}}|^2 = |\theta_{\mathbf{E}}|^2 . \tag{10}$$

Therefore the magnitude of each vector $\theta_{\mathbf{ES}}$, $\theta_{\mathbf{EV}}$ and $\theta_{\mathbf{E}}$ is independent of time.

Let $\Theta_{\rm Lab}$ be the polar angle of $\theta_{\mathbf{ES}}$ in the laboratory coordinate system. From (9), we find $\cos\Theta_{\rm Lab} = c_\delta c_a$. We may classify the apparent time variation into two typical cases, $\eta \le \Theta_{\rm Lab}$ and $\eta \ge \Theta_{\rm Lab}$. Figure 3 shows the two cases for the apparent time variation of $\theta_{\mathbf{E}}$ in the laboratory coordinate system. Let Φ_E be the azimuthal angle of $\theta_{\mathbf{E}}$ in the laboratory coordinate system. In the case (a) $\eta \le \Theta_{\rm Lab}$, Φ_E varies in the region of $(\Phi_E^{\max} - \Phi_E^{\min}) \le \pi$. On the other hand, in the case (b) $\eta \ge \Theta_{\rm Lab}$, Φ_E varies in the whole

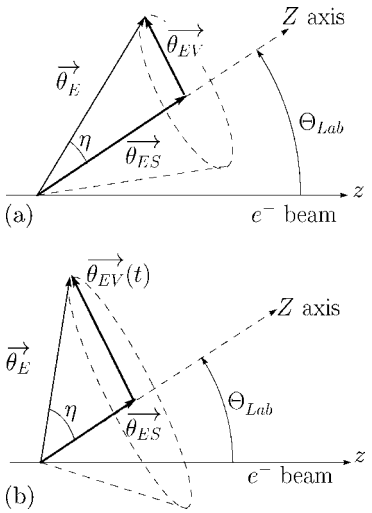

Fig. 3. Two typical time variation of $\theta_{\mathbf{E}}$ in the laboratory frame. **a** for $\eta \le \Theta_{\rm Lab}$ and **b** for $\eta \ge \Theta_{\rm Lab}$, where $\cos\Theta_{\rm Lab} = c_\delta c_a$

region. Therefore we may expect that some typical differences exist between the case (a) and (b) in the angular distribution for a process, for example $e^-e^+ \to \gamma\gamma$, which are affected by the space-time noncommutativity.

The magnetic-like component $\theta_{\mathbf{B}}$ is also parametrized by the same way. In general, however, both the direction and the magnitude of $\theta_{\mathbf{B}}$ are different from those of $\theta_{\mathbf{E}}$. Therefore $\theta_{\mu\nu}$ can be parameterized by six parameters, four angles and two magnitudes of $\theta_{\mathbf{E}}$ and $\theta_{\mathbf{B}}$, $\theta_E = |\theta_{\mathbf{E}}|$ and $\theta_B = |\theta_{\mathbf{B}}|$. In the primary coordinate system,

$$\theta_{\mathbf{E}} = \theta_E \left(\mathbf{e_X} \sin\eta_E \cos\xi_E + \mathbf{e_Y} \sin\eta_E \sin\xi_E + \mathbf{e_Z} \cos\eta_E\right) , \tag{11}$$

$$\theta_{\mathbf{B}} = \theta_B \left(\mathbf{e_X} \sin\eta_B \cos\xi_B + \mathbf{e_Y} \sin\eta_B \sin\xi_B + \mathbf{e_Z} \cos\eta_B\right) . \tag{12}$$

By using (5), we can obtain the expression of $\theta_{\mathbf{E}}$ and $\theta_{\mathbf{B}}$ in the laboratory coordinate system. We should take θ_E and θ_B as model parameters and the corresponding energy scale may be defined as $\Lambda_E = 1/\sqrt{\theta_E}$ and $\Lambda_B = 1/\sqrt{\theta_B}$.

3 $e^-e^+ \to \gamma\gamma$ in NCQED

A field theory in noncommutative space-time can be described equivalently by a field theory with commutative space-time variables in which every products of fields are replaced by the star product of fields. The star product is defined by

$$f \star g(x) = \exp\left(\frac{\mathrm{i}}{2}\partial_y^\mu \theta_{\mu\nu} \partial_z^\nu\right) f(y) g(z)\Big|_{y=z=x} , \tag{13}$$

where x, y and z are ordinary commutative variables.

NCQED action [9] is then given by

$$S = \int \mathrm{d}^4x \left(-\frac{1}{4} F^{\mu\nu} \star F_{\mu\nu} + \mathrm{i}\bar\Psi \gamma^\mu \star D_\mu \Psi - m\bar\Psi\Psi\right) , \tag{14}$$

where $F^{\mu\nu} = \partial^\mu A^\nu - \partial^\nu A^\mu - \mathrm{i}e(A^\mu \star A^\nu - A^\nu \star A^\mu)$. The covariant derivative of the matter fields is given by $D_\mu\Psi = \partial_\mu\Psi - \mathrm{i}eA_\mu \star \Psi$. We need nonlinear terms in field strength $F_{\mu\nu}$ to keep NCQED action invariant under noncommutative $\mathrm{U}(1)_\star$ gauge transformation,

$$A_\mu \to A'_\mu = U(x) \star A_\mu \star U^{-1}(x) - \frac{\mathrm{i}}{e}(\partial_\mu U(x)) \star U^{-1}(x) , \tag{15}$$

$$\Psi(x) \to \Psi'(x) = U(x) \star \Psi(x) , \tag{16}$$

$$\bar\Psi(x) \to \bar\Psi'(x) = \bar\Psi(x) \star U^{-1}(x) , \tag{17}$$

where

$$U(x) = \exp(\mathrm{i}\alpha(x))_\star \equiv \sum_{n=0} \frac{(\mathrm{i}\alpha(x)\star)^n}{n!} \tag{18}$$

and $U(x) \star U^{-1}(x) = U^{-1}(x) \star U(x) = 1$.

In NCQED, we consider the pair annihilation process $e^-(k_1)e^+(k_2) \to \gamma(p_1)\gamma(p_2)$ at future e^-e^+ linear colliders. Each momentum is taken to be

$$k_1^\mu = \frac{\sqrt{s}}{2}(1,0,0,1) , \quad k_2^\mu = \frac{\sqrt{s}}{2}(1,0,0,-1) ,$$
$$p_1^\mu = \left(\frac{\sqrt{s}}{2}, \mathbf{p}\right) , \quad p_2^\mu = \left(\frac{\sqrt{s}}{2}, -\mathbf{p}\right) , \tag{19}$$

where $\mathbf{p} = (\sqrt{s}/2)(s_\theta c_\phi, s_\theta s_\phi, c_\theta)$. θ and ϕ are the polar and the azimuthal angles of final state photon in the laboratory coordinate system. The differential cross-section for $e^-(k_1)e^+(k_2) \to \gamma(p_1)\gamma(p_2)$ in the center of mass system is given by

$$\frac{\mathrm{d}\sigma_{\mathrm{obs}}}{\mathrm{d}\cos\theta\,\mathrm{d}\phi} = \frac{\alpha^2}{2s}\left(\frac{t}{u} + \frac{u}{t} - 4\frac{t^2+u^2}{s^2}\sin^2\Delta_{\mathrm{NC}}\right) , \tag{20}$$

$$\Delta_{\mathrm{NC}} = \frac{p_1^\mu \theta_{\mu\nu} p_2^\nu}{2} = -\left(\frac{s}{4}\right)\frac{\theta_{\mathbf{E}} \cdot \mathbf{p}}{|\mathbf{p}|} , \tag{21}$$

where s, t and u are usual Mandelstam variables, $s = (k_1 + k_2)^2$, $t = (k_1 - p_1)^2$ and $u = (k_1 - p_2)^2$. Since two photons in the final state are identical, we cannot distinguish two configuration (θ, ϕ) and $(\pi - \theta, \pi + \phi)$. Equation (20) is defined in the region $0 \le \cos\theta < 1$ and $0 \le \phi \le 2\pi$. The $\theta_{\mathbf{E}}$ is given in (7), (8) and (9). When $\Delta_{\mathrm{NC}} = 0$, the differential cross-section (20) reduces to that in QED.

It is easy to show from (20) and (21) that $\Delta_{\mathrm{NC}}(\pi - \theta, \pi + \phi) = -\Delta_{\mathrm{NC}}(\theta, \phi)$ and

$$\frac{\mathrm{d}\sigma_{\mathrm{obs}}}{\mathrm{d}\cos\theta\,\mathrm{d}\phi}(\Delta_{\mathrm{NC}}) = \frac{\mathrm{d}\sigma_{\mathrm{obs}}}{\mathrm{d}\cos\theta\,\mathrm{d}\phi}(-\Delta_{\mathrm{NC}}) . \tag{22}$$

Moreover, this imply that the differential cross-section (20) is symmetric for the change of the sign of $\theta_{\mathbf{E}}$, $\theta_{\mathbf{E}} \leftrightarrow -\theta_{\mathbf{E}}$. Therefore we cannot distinguish between (η, ξ) and $(\pi - \eta, \pi + \xi)$ by observing the process $e^-e^+ \to \gamma\gamma$. There is twofold ambiguity for the determination of (η, ξ).

We can see from (20) that the NCQED effect on the differential cross-section of $e^-e^+ \to \gamma\gamma$ always gives the negative contribution; moreover, from (21) we find

$$|\Delta_{\mathrm{NC}}| = \max(\Delta_{\mathrm{NC}}) = \frac{s}{4}\theta_E \quad \text{if} \quad \mathbf{p} \parallel \theta_{\mathbf{E}} , \tag{23}$$

$$\Delta_{\mathrm{NC}} = 0 \quad \text{if} \quad \mathbf{p} \perp \theta_{\mathbf{E}} . \tag{24}$$

This means that, when we compare the NCQED prediction with the QED prediction, the deficit of the differential cross-section appears around the specific direction in which $\mathbf{p}$ is almost parallel to $\theta_{\mathbf{E}}$. Furthermore, such a specific direction varies with time in the laboratory coordinate system, as we have discussed in the previous section. Therefore, in general, observables for $e^-e^+ \to \gamma\gamma$ in the laboratory coordinate system have time dependence even for the total cross-section.

We may consider that cross-sections measured at collider experiments are the mean values averaged over the operation time of each experiment. And such a mean value should be compared with NCQED prediction averaged

over time. Taking into consideration that the period of time variation of the observables in NCQED is the sidereal day $T_{\rm day}$, we introduce the time averaged observables as follows:

$$\left\langle \frac{\mathrm{d}\sigma}{\mathrm{d}\cos\theta\,\mathrm{d}\phi} \right\rangle_T \equiv \frac{1}{T_{\rm day}} \int_0^{T_{\rm day}} \frac{\mathrm{d}\sigma_{\rm obs}}{\mathrm{d}\cos\theta\,\mathrm{d}\phi}\,\mathrm{d}t\,, \quad (25)$$

$$\left\langle \frac{\mathrm{d}\sigma}{\mathrm{d}\cos\theta} \right\rangle_T \equiv \frac{1}{T_{\rm day}} \int_0^{T_{\rm day}} \frac{\mathrm{d}\sigma_{\rm obs}}{\mathrm{d}\cos\theta}\,\mathrm{d}t\,, \quad (26)$$

$$\left\langle \frac{\mathrm{d}\sigma}{\mathrm{d}\phi} \right\rangle_T \equiv \frac{1}{T_{\rm day}} \int_0^{T_{\rm day}} \frac{\mathrm{d}\sigma_{\rm obs}}{\mathrm{d}\phi}\,\mathrm{d}t\,, \quad (27)$$

$$\langle\sigma\rangle_T \equiv \frac{1}{T_{\rm day}} \int_0^{T_{\rm day}} \sigma_{\rm obs}\,\mathrm{d}t\,, \quad (28)$$

where

$$\frac{\mathrm{d}\sigma_{\rm obs}}{\mathrm{d}\cos\theta} \equiv \int_0^{2\pi} \mathrm{d}\phi \frac{\mathrm{d}\sigma_{\rm obs}}{\mathrm{d}\cos\theta\,\mathrm{d}\phi}\,, \quad (29)$$

$$\frac{\mathrm{d}\sigma_{\rm obs}}{\mathrm{d}\phi} \equiv \int_0^{1-\epsilon} \mathrm{d}(\cos\theta) \frac{\mathrm{d}\sigma_{\rm obs}}{\mathrm{d}\cos\theta\,\mathrm{d}\phi}\,, \quad (30)$$

$$\sigma_{\rm obs} \equiv \int_0^{1-\epsilon} \mathrm{d}(\cos\theta) \int_0^{2\pi} \mathrm{d}\phi \frac{\mathrm{d}\sigma_{\rm obs}}{\mathrm{d}\cos\theta\,\mathrm{d}\phi}\,. \quad (31)$$

The polar angle cut is denoted by ϵ ($0 \le \epsilon \le 1$).

Note that we have integrated out the ξ dependence of the observables by taking average over time, since ξ play a role of initial phase for time evolution. Therefore θ_E and the angle η may be determined by the time averaged observables.

4 Numerical results

We show several characteristic results in NCQED and also discuss how to probe $\theta_{\mathbf{E}}$ by using observables in the laboratory coordinate system. We set the laboratory coordinate system by taking $(\delta, a) = (\pi/4, \pi/4)$, which is close to the OPAL experiment at LEP. The cut for $\cos\theta$ is taken $\epsilon = 0.2$.

4.1 Azimuthal angle distribution

Anisotropy of azimuthal angle distribution of $e^-e^+ \to \gamma\gamma$ is predicted in NCQED even if we consider the time averaged distribution $\langle \mathrm{d}\sigma/\mathrm{d}\phi\rangle_T$. Figure 4 shows $\langle \mathrm{d}\sigma/\mathrm{d}\phi\rangle_T$ for $\theta_E = (500\,\mathrm{GeV})^{-2}$ and several values of η. We take $\sqrt{s} = 500\,\mathrm{GeV}$.

When $\eta = 0$ and π, there is no apparent time variation in the laboratory frame, because $\theta_{\mathbf{EV}} = 0$. In this case, the graph of $\langle \mathrm{d}\sigma/\mathrm{d}\phi\rangle_T$ show large variation as compared with that for other values of η. To take the time average weaken the variation of $\langle \mathrm{d}\sigma/\mathrm{d}\phi\rangle_T$ for $\eta \neq 0, \pi$.[3]

[3] If $\theta_{\mathbf{E}}$ were constant vector in the laboratory coordinate system, the azimuthal angle distribution should be different from Fig. 4, except for the case $\eta = 0, \pi$. In case that $\theta_{\mathbf{E}}$ is a constant vector in the laboratory frame, the results have been shown in [20].

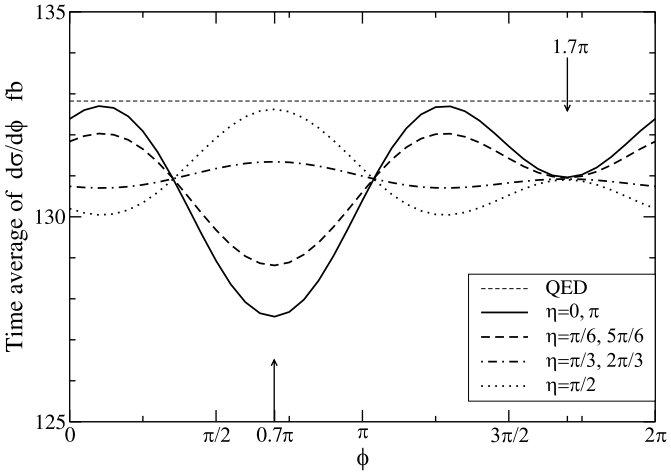

Fig. 4. Time averaged azimuthal angle distribution for $\eta = 0$, $\pi/6$, $\pi/3$, $\pi/2$, $2\pi/3$, $5\pi/6$, π. We set the laboratory coordinate system by taking $(\delta, a) = (\pi/4, \pi/4)$. We take $\sqrt{s} = 500\,\mathrm{GeV}$ and $\theta_E = (500\,\mathrm{GeV})^{-2}$

We see from Fig. 4 that the curves of $\langle \mathrm{d}\sigma/\mathrm{d}\phi\rangle_T$ are sensitive to the value of η around $\phi \simeq 0.7\pi$ and also almost independent of the value of η around $\phi \simeq 1.7\pi$. Furthermore $\langle \mathrm{d}\sigma/\mathrm{d}\phi\rangle_T$ is almost flat around $\phi \simeq 1.7\pi$ for any η.

Those specific angles 0.7π and 1.7π can be interpreted as the azimuthal angle of $\theta_{\mathbf{ES}}$ and $-\theta_{\mathbf{ES}}$ in the laboratory coordinate system. In other words, those are the azimuthal angles of the North Pole and the South Pole of the celestial sphere. Since we take $(\delta, a) = (\pi/4, \pi/4)$, the azimuthal angle ϕ^N_{ES} of $\theta_{\mathbf{ES}}$ can be derived from (9) as follows

$$\cos\phi^N_{ES} = \frac{-c_\delta s_a}{\sqrt{1 - c_\delta^2 c_a^2}} = -\frac{1}{\sqrt{3}}\,,$$
$$\sin\phi^N_{ES} = \frac{s_\delta}{\sqrt{1 - c_\delta^2 c_a^2}} = \sqrt{\frac{2}{3}}\,, \quad (32)$$

then $\phi^N_{ES} \simeq 0.7\pi$ and the azimuthal angle of $-\theta_{\mathbf{ES}}$ is given by $\phi^N_{ES} + \pi \simeq 1.7\pi$.

We also see from Fig. 4 that each input η and $\pi - \eta$ gives the same distribution of $\langle \mathrm{d}\sigma/\mathrm{d}\phi\rangle_T$. This is because the differential cross-section of $e^-e^+ \to \gamma\gamma$ is symmetric for $\theta_{\mathbf{E}} \leftrightarrow -\theta_{\mathbf{E}}$.

We may determine η, except for the twofold ambiguity between η and $\pi - \eta$, by fitting the shape of $\langle \mathrm{d}\sigma/\mathrm{d}\phi\rangle_T$, especially at around $\phi \simeq \phi^N_{ES} = 0.7\pi$. We may also determine θ_E almost independently of η by measuring the deficit of $\langle \mathrm{d}\sigma/\mathrm{d}\phi\rangle_T$ compared with the QED prediction around $\phi \simeq 1.7\pi$.

4.2 Time dependent total cross-section

In order to determine ξ, we need to trace the apparent time variation of observables due to the earth's rotation. Since the total cross-section $\sigma_{\rm obs}$ depends on θ_E, η and also ξ, we may expect that θ_E, η and ξ could be determined by measuring the time variation of $\sigma_{\rm obs}$ precisely, except for the twofold ambiguity between (η, ξ) and $(\pi - \eta, \xi + \pi)$.

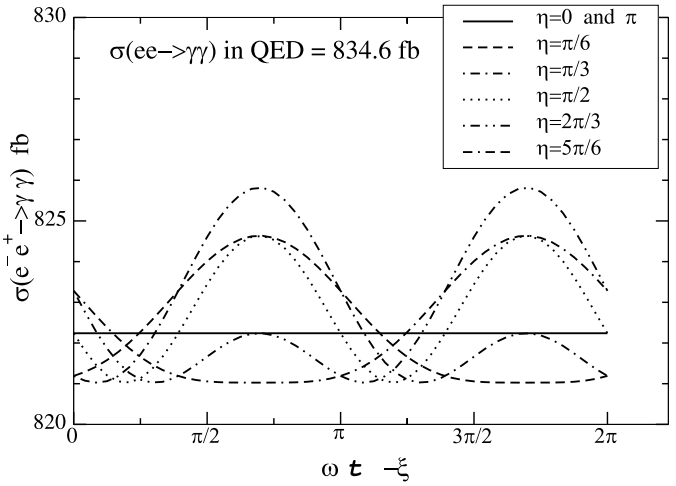

Fig. 5. Apparent time variation of total cross section for $\eta = 0, \pi/6, \pi/3, \pi/2, 2\pi/3, 5\pi/6$ and π. We take $(\delta, a) = (\pi/4, \pi/4)$, $\sqrt{s} = 500$ GeV and $\theta_E = (500\,\mathrm{GeV})^{-2}$

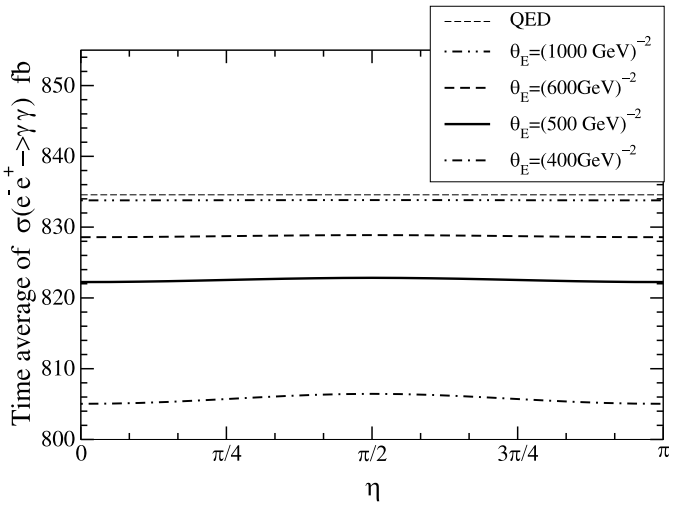

Fig. 6. Time averaged total cross-section of $e^-e^+ \to \gamma\gamma$ for $\theta_E = (400\,\mathrm{GeV})^{-2}$, $(500\,\mathrm{GeV})^{-2}$, $(600\,\mathrm{GeV})^{-2}$ and $(1000\,\mathrm{GeV})^{-2}$ are shown. Horizontal axis is taken to be angle η. QED result is also shown. We take $(\delta, a) = (\pi/4, \pi/4)$ and $\sqrt{s} = 500$ GeV

Figure 5 shows $\sigma_{\rm obs}$ as a function of $\omega t - \xi$ for $\theta_E = (500\,\mathrm{GeV})^{-2}$ and for several values of η. We can see from Fig. 5 that $\sigma_{\rm obs}$ is sensitive to the η. If the time variation of total cross-section is observed, we could determine both the magnitude and the direction of $\boldsymbol{\theta_E}$ by fitting the NCQED prediction of $\sigma_{\rm obs}$ with the data in the three parameter space (θ_E, η, ξ). The magnitude θ_E and the angle η may be determined by fitting both the magnitude and the time variation of $\sigma_{\rm obs}$. The ξ may be determined by the measurement of the phase of time evolution of $\sigma_{\rm obs}$.

Although we may determine $\boldsymbol{\theta_E}$ by tracing the time variation of the differential cross-section of $e^-e^+ \to \gamma\gamma$ instead of total cross-section, we can imagine that such an experiment needs very large luminosity. This is because we must divide not only the phase space but also the time distribution into many bins, in order to trace the time variation. Therefore, in the determination of θ_E, η and ξ, we had better probe the time variation of total cross-section in the early stage of experiments at e^-e^+ linear colliders. It should be noted, however, that once a positive signal is identified, the expected time variation can be tested in detail not only at linear collider experiments but also at all the other on-going and completed experiments.

4.3 $\langle \mathrm{d}\sigma/\mathrm{d}\phi \rangle_T$ vs. $\sigma_{\rm obs}$

We can see from Figs. 4 and 5 that $\langle \mathrm{d}\sigma/\mathrm{d}\phi \rangle_T$ and $\sigma_{\rm obs}$ show opposite behavior for each input value of η. For example, when $\eta = 0$ or π, we may observe large variation of azimuthal angle distribution $\langle \mathrm{d}\sigma/\mathrm{d}\phi \rangle_T$. In this case, we find no time variation of $\sigma_{\rm obs}$. On the contrary, when $\eta = \pi/3$ or $2\pi/3$, since the variation of $\langle \mathrm{d}\sigma/\mathrm{d}\phi \rangle_T$ is very small, we may observe the flat distribution in the experiments. In this case, we find large time variation of $\sigma_{\rm obs}$. Therefore we may expect that non-uniform distribution due to the NCQED effect should appear in $\langle \mathrm{d}\sigma/\mathrm{d}\phi \rangle_T$ and/or $\sigma_{\rm obs}$ for any values of η and ξ, if θ_E is large enough.

4.4 Time averaged total cross-section

Finally, we consider what we can measure by the time averaged total cross-section $\langle \sigma \rangle_T$. Figure 6 shows $\langle \sigma \rangle_T$ as a function of η. It is easy to see that $\langle \sigma \rangle_T$ is almost independent of η. Therefore if a deficit of $\langle \sigma \rangle_T$ is observed, we can determine θ_E independently of η.

On the other hand, if we observe no signal, we may obtain the upper limit on θ_E. The 1σ deviation for total cross-section in QED, $\sigma_{\rm QED}$, can be estimated by $\sqrt{\sigma_{\rm QED}/L}$. For $\sqrt{s} = 500$ GeV and $\epsilon = 0.2$, we have $(28.89/\sqrt{L})$ where L is the luminosity given in fb^{-1}. In this case, an expected 95%CL upper limit on θ_E is found to be

$$\theta_E \lesssim (600\,\mathrm{GeV})^{-2} \quad \text{for} \quad L = 100\,\mathrm{fb}^{-1}. \tag{33}$$

Furthermore, since $|\sigma_{\rm QED} - \langle \sigma \rangle_T| \propto (s\theta_E)^2$ for $|s\theta_E| < 1$, we may estimate 95%CL upper limit on θ_E for arbitrary L from (33) as follows:

$$\theta_E \lesssim (600\,\mathrm{GeV})^{-2} \left(\frac{100\,\mathrm{fb}^{-1}}{L}\right)^{1/4}. \tag{34}$$

For example, we find $\theta_E \lesssim (800\,\mathrm{GeV})^{-2}$ when L=1000 fb^{-1}.

5 Conclusion and remarks

We have presented phenomenological formulation of the apparent time variation of noncommutativity parameter $\theta_{\mu\nu}$ in the laboratory coordinate system. In our framework, the laboratory coordinate system is chosen as the standard one for collider experiments, and the primary coordinate system fixed to the celestial sphere have been introduced. We have shown the transformation formula between the primary and the laboratory coordinate system, and also

shown the expression of $\theta_{\mathbf{E}}$ in the laboratory coordinate system. The formulation presented in this paper is applicable to the study of any models which predict an intrinsic direction of the space-time [9, 44, 45].

As an example, we have applied our formalism to NCQED and discussed how we can measure $\theta_{\mathbf{E}}$ at future e^-e^+ linear collider experiments by the process $e^-e^+ \to \gamma\gamma$. The $\theta_{\mathbf{E}}$ have been parameterized by θ_E, η and ξ in the primary coordinate system. We have shown that $\theta_{\mathbf{E}}$ may be determined by the detailed study of the time dependent total cross-section, though twofold ambiguity in the parameter space (η, ξ) remains. To determine ξ, we need to probe the phase of the time evolution of $\sigma_{\rm obs}$. If there is no signal, we can obtain the upper limit on θ_E independently of the direction of $\theta_{\mathbf{E}}$.

So far we have considered one experiment with $(\delta, a)=(\pi/4,\ \pi/4)$. If there are several detector sites in the e^-e^+ collider experiment and the direction of e^- beam in each site is set to be along to the different direction, such as the four LEP experiments, then the angular distributions of $e^-e^+ \to \gamma\gamma$ and the time variation of observables should behave differently in each experiment. This is because the direction of $\theta_{\mathbf{ES}}$ in the laboratory coordinate system at one detector site differs from that at other detector sites. Therefore we can expect that the combined analysis of several experiments with the different (δ, a) plays an important role in the attempt to probe the space-time noncommutativity.

Finally, we would like to make some comments on the determination of the magnetic-like component $\theta_{\mathbf{B}}$. Since the process $e^-e^+ \to \gamma\gamma$ is independent of $\theta_{\mathbf{B}}$, to determine $\theta_{\mathbf{B}}$, we must consider other processes relevant to $\theta_{\mathbf{B}}$, for example $e^-\gamma \to e^-\gamma$ process which depend on both $\theta_{\mathbf{E}}$ and $\theta_{\mathbf{B}}$. The process $\gamma\gamma \to \gamma\gamma$ may also be available to determine $\theta_{\mathbf{B}}$. By combining the results from those processes, we may determine $\theta_{\mathbf{E}}$ and $\theta_{\mathbf{B}}$. We postpone the study of this matter to future studies.

Acknowledgements. The author thanks O. Kamei and A. Sugamoto for reading the manuscript and useful comments, and K. Hagiwara and T. Kawamoto for useful discussion and comments. The author also thanks I. Watanabe for useful comments on the usefulness of the X axis defined by the vernal equinox $\Upsilon_{2000.0}$.

References

1. H.S. Snyder, Phys. Rev. **71**, 38 (1947)
2. H.S. Snyder, Phys. Rev. **72**, 68 (1947)
3. A. Connes, M.R. Douglas, A. Schwarz, J. High Energ. Phys. **02**, 0003 (1998)
4. N. Seiberg, E. Witten, J. High Energ. Phys. **09**, 032 (1999)
5. S.M. Carroll et al., Phys. Rev. Lett. **87**, 141 601 (2001)
6. V.A. Kostelecký, C.D. Lane, Phys. Rev. D **60**, 116 010 (1999)
7. V.A. Kostelecký, Phys. Rev. D **61**, 016 002 (1999)
8. D. Colladay, V.A. Kostelecký, Phys. Lett. B **511**, 209 (2001)
9. M. Hayakawa, Phys. Lett. B **478**, 394 (2000)
10. M. Hayakawa, hep-th/9912167
11. J.M. Gracia-Bondía, C.P. Martín, Phys. Lett. B **479**, 321 (2000)
12. F. Ardalan, N. Sadooghi, Int. J. Mod. Phys. A **16**, 3151 (2001)
13. M.M. Sheikh-Jabbari, Phys. Rev. Lett. **84**, 5265 (2000)
14. I.F. Riad, M.M. Sheikh-Jabbari, J. High Energ. Phys. **08**, 045 (2000)
15. X.J. Wang, M.L. Yan, J. High Energ. Phys. **03**, 047 (2002)
16. N. Chair, M.M. Sheikh-Jabbari, Phys. Lett. B **504**, 141 (2001)
17. M. Haghighat, S.M. Zebarjad, F. Loran, Phys. Rev. D **66**, 016 005 (2002)
18. M. Chaichian, M.M. Sheikh-Jabbari, A. Tureanu, Phys. Rev. Lett. **86**, 2716 (2001)
19. H. Falomir et al., Phys. Rev. D **66**, 045 018 (2002)
20. J.L. Hewett, F.J. Petriello, T.G. Rizzo, Phys. Rev. D **64**, 075 012 (2001)
21. H. Arfaei, M.H. Yavartanoo, hep-th0010244
22. P. Mathews, Phys. Rev. D **63**, 075 007 (2001)
23. S. Godfrey, M.A. Doncheski, Phys. Rev. D **65**, 015 005 (2002)
24. S. Godfrey, M.A. Doncheski, eConf C010630, P313 (2001)
25. S. Godfrey, M.A. Doncheski, hep-ph/0111147
26. T.G. Rizzo, Int. J. Mod. Phys. A **18**, 2797 (2003)
27. I. Mocioiu, M. Pospelov, R. Roiban, Phys. Lett. B **489**, 390 (2000)
28. C.E. Carlson, C.D. Carone, R.F. Lebed, Phys. Lett. B **518**, 201 (2001)
29. S. Baek et al., Phys. Rev. D **64**, 056 001 (2001)
30. I. Hinchliffe, N. Kersting, Phys. Rev. D **64**, 116 007 (2001)
31. H. Grosse, Y. Liao, Phys. Lett. B **520**, 63 (2001)
32. A. Mazumdar, M.M. Sheikh-Jabbari, Phys. Rev. Lett. **87**, 011 301 (2001)
33. N. Kersting, Phys. Lett. B **527**, 115 (2002)
34. W. Behr et al., hep-ph/0202121
35. E.O. Iltan, JHEP **0211**, 029 (2002)
36. E.O. Iltan, New J. Phys. **4**, 54 (2002)
37. E.O. Iltan, Phys. Rev. D **66**, 034 011 (2002)
38. H. Grosse, Y. Liao, Phys. Rev. D **64**, 115 007 (2001)
39. I. Hinchliffe, N. Kersting, Y.L. Ma, hep-ph/0205040
40. G.F. Smoot et al., Astrophys. J. **371**, L1 (1991)
41. A. Kogut et al., Astrophys. J. **419**, 1 (1993)
42. T. Kawamoto, private communication
43. for example, see Particle Data Group, K. Hagiwara et al., Phys. Rev. D **66**, 010 001 (2002)
44. other than NCQED, for example, A. Sugamoto, Prog. Theor. Phys. **107**, 793 (2002)
45. G.C. Cho, E. Izumi, A. Sugamoto, Phys. Rev. D **66**, 116 009 (2002)